3
Quantification of Organofluorine-Protein Interactions

3.1 INTRODUCTION

^{19}F NMR based screening methods provide mechanistic analysis of molecular interaction involving fluorine containing fragments that leads to design of potential drugs, enzyme inhibitors and agrochemicals by exploiting the unique functionality of the organofluorines [Berkowitz et al., 2009]. The recent upsurge in the synthesis and use of organofluorines in agrochemistry and pharmaceuticals as discussed in Chapter 1 [Champagne et al., 2015] has necessitated the applications of ^{19}F NMR as one of the major analytical tools providing atomic level understanding of fluorine containing ligand-macromolecule interactions. Besides characterization of the said molecular interactions, such analysis offers the knowledge about the indirect side effects of the organofluorines which is not well documented and need to be explored continuously. This knowledge can be used as a secondary factor to be taken into consideration while selecting suitable fluorinated molecules and their doses in agriculture and medicine. In principle, both ligand observed and protein observed NMR methods are capable to provide comprehensive understanding of these molecular systems. In general multidimensional protein based NMR methods requiring isotopically labelled protein samples become an expensive affair compared to the corresponding ligand observed methods with respect to both machine time and sample preparation. Moreover, in case of multifluorinated ligands the two-dimensional (2D) experiments are difficult to realize due to radiofrequency excitation pulse bandwidth issues indicating one dimensional ligand observed NMR methods as more attractive tools combating some of these hurdles with ease.

The present chapter therefore attempts to establish the applicability of one-dimensional (1D) ^{19}F ligand observed NMR approaches for systematic analysis of organofluorine and protein interaction in solution highlighting the pros and cons of a few majorly employed 1D NMR methods, namely, CPMG extracting transverse relaxation rates, diffusion analysis monitoring self-diffusion constants of the ligands under investigation and STD NMR revealing group epitope maps wherever possible. The chapter specifically addresses the binding interaction of a selected set of organofluorine ligands with two biologically important proteins: (i) serum albumin (SA) and (ii) trypsin. Interaction analysis of the organofluorine with SA (plasma protein) attracts attention due to abundant availability of SA in the body that may affect the metabolism, circulation, and excretion mechanism of these molecules within the body [Sudhamalla et al., 2010]. On the other hand, trypsin is a digestive enzyme that also plays vital role in the regulation of many biochemical and biologically relevant processes. Besides SA, it is also considered as a model binding protein to screen a number of fragments that can be further used in drug discovery processes. The chapter reports the experimental findings in two parts: the first part (Part I) addresses the binding of fluorine containing ligands with SA while the second part (Part II) reveals ligand interaction with trypsin.

3.1.1 Proteins under investigation: Literature background

Serum albumin (SA), are the most abundant globular protein in blood plasma and functions as a major carrier protein in our blood. SA is rich in multiple lipophilic binding sites at its surface, and it interacts with various exogenous and endogenous substances in blood plasma by forming non-covalent complexes. It also serves as the major transporter for compounds to their target organs and tissues. Human serum albumin (HSA) and Bovine serum albumin (BSA, commonly used due to 75% structural analogy with HSA) are the most extensively studied model proteins in several biophysical, and biochemical investigations carried out for protein-

ligand interactions analysis employing various *in vitro* and *in vivo* methods [Lee and Lee, 1995; Ni et al., 2012]. SA is a single-chain, non-glycosylated polypeptide with a molecular weight of 67 kDa, containing 585 amino acids [Raoufinia et al., 2016]. SA is an all helical protein and has three domains (I-III), with each domain having subdomains (A and B). SA carries out many essential physiological functions, such as the regulation of colloidal osmotic pressure and the transport of endogenous compounds *viz*., fatty acids (FAs), hormones, bile acids, amino acids, metal ions, and other metabolites [Sudhamalla et al., 2010]. SA being a multifunctional protein also possesses catalytic properties against a variety of xenobiotic substrate, and known for its pseudo-enzymatic activity [Goncharov et al, 2015]. SA is known as a major pharmacokinetic modulator of ligand (drug) action, and the investigation of ligand-SA complexes will enable understanding of ligand ADMET (adsorption, distribution, metabolism, excretion, and toxicological properties) and therapeutic effectiveness.

Trypsin is one of the important class of enzyme that serves as an important target in contemporary medicinal chemistry [Gonclaves et al., 2010; Talhout and Engberts, 2001]. Trypsin contains 223 amino acid residues with six disulfide bridges that hold the individual chains together. It has two domains, with nearly the same size with six antiparallel β-sheet. Being a water-soluble serine protease, it helps in digestion of food proteins, protein maturation, apoptosis, control of blood pressure, immune response, hemostasis, blood coagulation, and signal transduction [Ren et al., 2019]. Also, it is a regulator of many other digestive proteases [Shuai et al., 2014]. The inhibition of trypsin activity can lead to reduced absorption of the nutrients [Gonc et al., 2011]. Many pathological changes in the human body and respective diseases are related to malfunctioning of the enzymatic activity of trypsin due to change in its structural conformation in the presence of a foreign substance. Screening of the compounds that (a) can specifically interact with a protein of pharmacological interest like trypsin or (b) can act as selective inhibitors for uncontrolled serine proteases will be useful for clinical applications as drugs [Bohm and Klebe, 1996; Ohba et al., 1996; Talhout and Engberts, 2001]. Further, in case of accidental intake of any contaminant that has the potential to affect the activity of the enzyme *in vivo* and may act as enzyme disruptor can also be analyzed through such screening processes [Liu et al., 2012; Saadati and Mizrael, 2016]. Therefore, due to the importance of trypsin in the digestive system, trypsin can serve as an indirect binding target for the aforesaid molecules [Wang and Zhang, 2014].

The interaction analysis of SA and trypsin with various exogenous substances or ligands and inhibition kinetics of trypsin have been addressed in literature by employing multi-spectroscopic methods [Gonçalves et al., 2010; Gonçalves et al., 2011; Liu et al., 2015; Liu et al., 2017; Shi et al., 2017; Wang et al., 2016; Wang and Zhang, 2014; Wang et al., 2015; Wu et al., 2017, 2018; Zhang et al., 2014]. The screening of various fluorinated drugs/inhibitors with a differential binding affinity towards SA, trypsin and related proteases has also been conducted employing ^{19}F NMR High throughput screening (HTS) methods like FAXS and FABS, ^{19}F hyperpolarized NMR, relaxation, relaxation dispersion CPMG (RD-CPMG), diffusion, STD and different other notable methods [Berkowitz et al., 2009; Buratto et al., 2016; Dalvit, 2007; Grembecka and Cierpicki, 2015; Kim and Hilty, 2015; Kim et al., 2018; Lee et al., 2012; Min, 2014; Moschen et al., 2016; Papeo et al., 2007; Price et al., 2002; Stockman and Dalvit, 2002]. The literature survey indicated that the molecular interaction of organofluorine and their metabolites with SA and trypsin is limited and therefore should be examined.

3.1.2 Organofluorine ligands under investigation: Literature background

The present chapter focuses to study the following fluorinated molecules used as drug in the commercial markets along with fluorinated molecular fragments or metabolites. Figure 3.1 (a) represents the chemical structures of these fluorochemicals.

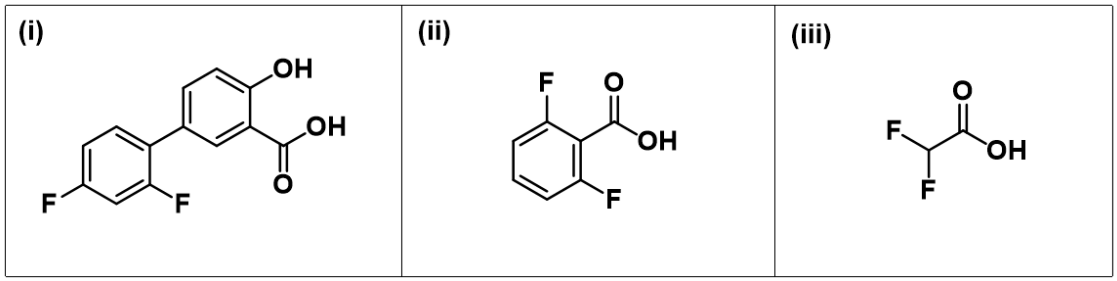

Figure 3.1 (a): Molecular structure of the fluorochemicals *viz.*, (i) diflunisal (DFL) (ii) 2, 6-difluorobenzoic acid (DFBA) and (iii) difluoroacetic acid (DFA) investigated in the current study.

- Dilfunisal (DFL, (5-(2, 4-difluorophenyl) salicylic acid) is a derivative of salicylic acid, a non-steroidal anti-inflammatory drug (NSAID) and is well known for binding to normal human plasma [Verbeeck et al., 1980]. A number of reports are available on the characterization of the interaction of DFL with SA implementing various analytical techniques, *i.e.*, potentiometric ion probe [Davilas et al., 2006], equilibrium dialysis [Verbeeck et al., 1980], $^{19}F–^{1}H$ STD [Sakuma et al., 2015], etc. Therefore, monitoring DFL interaction with HSA serves as a perfect model system to validate ^{19}F ligand-based experiments to analyze ligand-protein binding.

- 2,6-Difluorobenzoinc acid (DFBA) is one of the primary metabolites of pesticides belonging to benzoylphenylurea family *i.e.*, diflubenzuron, hexaflumuron etc. [Gattavecchia et al., 1981; Nimmo et al., 1990]. Further, DFBA has been used as a starting reagent in various synthetic routes to generate fluorine-containing molecules of importance such as number of potential PET agents for imaging cancer, namely 2,6-difluoro-N-(3-methoxy-1H-pyrazolo[3,4-b]pyridine-5-yl)-3 propylsulfonamidio) benzamide and methyl 2,6-difluorobenzoate [Wang et al., 2013] are derived from DFBA. It is well known that aqueous solubility is questionable in most cases of multi-fluorinated ligands. However, DFBA being a molecular fragment, exhibits excellent water solubility allowing protein interaction analysis to be carried out in aqueous media. In addition to that DFBA being metabolite of several pesticides may exert an adverse effect on binding to various biologically active proteins [Dahiya et al., 2017]. A well-characterized binding mechanism with soluble fragment would, therefore, allow understanding of the effect of the pesticide, or it may also help in developing lead molecules from these fragments that can be target-specific hit for challenging receptors [Gee et al., 2016; Harner et al., 2014]. Therefore, it becomes an interesting choice to monitor the interaction of DFBA with SA as well as with trypsin. Furthermore, DFBA-protein interaction is not yet discussed in any literature till date as per our knowledge. In the case of DFBA, we chose to work with BSA due to ease of commercial availability of BSA, cost-effectiveness, and homology with HSA [Verbeeck et al., 1980].

- Difluoroacetic acid (DFA) is one of the ultimate fluorinated degraded small fragments of insecticides like flupyradifurone (FPD) [Glaberman and Katrina, 2014]. No reports of interaction of DFA with any protein of interest are found in the literature. The study of organofluorine with trypsin can be useful to provide valuable insights for developing target-specific hits for the enzyme trypsin.

3.1.3 Methods in focus

In both Part I and Part II, 1D ^{19}F NMR ligand based experiments have been employed to obtain qualitative and quantitative description of the organofluorine-protein binding interactions. Preliminary qualitative evidences of binding are obtained by monitoring the

changes in chemical shift and line-broadening of fluorinated ligands in the absence and presence of the protein. ^{19}F relaxation and diffusion experiments are also employed to probe the interaction between organofluorine and protein by monitoring changes in relaxation time and self-diffusion coefficient.

In case of Part I, a set of competition binding experiments with well-known site markers of SA is also performed to identify the ligand binding sites on SA. Group Epitope Map (GEM) generated through ^{19}F–^{1}H and ^{1}H–^{1}H STD NMR experiments have also provided a qualitative description of the parts of ligand binding to the protein. For quantifying the binding strength, measurements of ligand transverse relaxation and translational diffusion behavior in absence and presence of the protein have been employed that allowed experimental extraction of the number of binding sites and the dissociation constants characterizing the complex formed between the test molecules and SA. Furthermore, ^{19}F constant time fast pulsing CPMG experiments are performed to extract the exchange rates between the free and the bound states of the fluorinated molecules employing a two-site exchange model. The lifetime of the drug-protein complex is further evaluated from the residence time determined from the reverse exchange rate. The residence time is also related to the dissociative half-life of the ligand-protein complex. It is a more powerful parameter compared to the affinity constant. It determines the pharmacological activities of the ligand by indicating *in vivo* duration of ligand efficacy, as suggested by Coopeland *et al.* [Copeland et al., 2007]. The outcome of Part I has suggested superior binding interaction of DFL with HSA as compared to that of DFBA with BSA. Figure 3.1 (b) presents a graphical illustration of the said organofluorine-SA binding interaction via ligand detected ^{19}F NMR methods [Chaubey and Pal, 2018].

In Part II, the interaction of the aromatic organofluorine molecules *viz.*, DFBA, DFL is further investigated with another model protein, trypsin employing similar 1D ^{19}F NMR methods in continuation of the part I. It is found that both DFBA and DFL did not exhibit any significant interaction with trypsin. Further, the investigation is extended to other aliphatic fluorinated molecule *i.e.* DFA. The findings of chemical shift, line-broadening, relaxation and diffusion confirmed that all investigated fluorochemicals containing carboxylic acid (CA) functional group, whether aromatic or aliphatic (DFL, DFBA, DFA) exhibited insignificant (undetectable) binding interaction with trypsin. Hence, it can be interpreted that the fluorinated molecules with only CA groups are not appropriate as potential inhibitors while screening for trypsin.

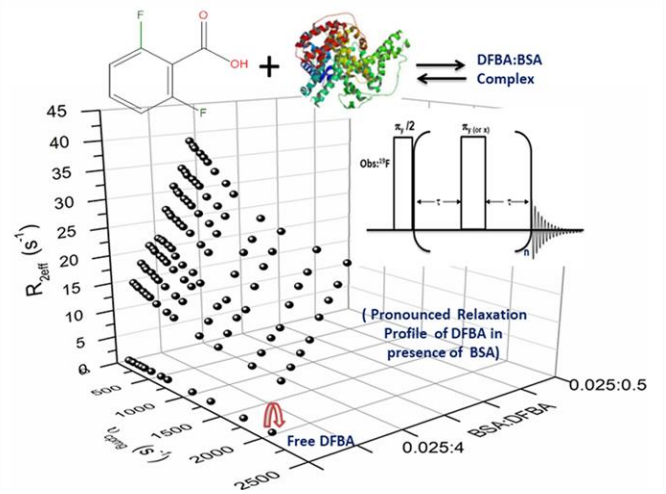

Figure 3.1 (b): Graphical representation of the current investigation showing changes in relaxation profile of test molecule on interaction with protein.

3.2 EXPERIMENTAL DETAILS

3.2.1 Sample preparation:

Solutions of SA, trypsin and DFBA are prepared in 0.05 M phosphate buffer at pH= 7.4. The final stock concentrations are 200 µM for SA, 100 µM for trypsin and 10 mM for DFBA. Stock solution of DFL with a concentration of 10 mM is prepared in dimethyl sulfoxide (DMSO) solvent to gain better solubility. The solutions used for NMR measurements in case of DFBA-BSA contained 25 µM of BSA and a varying concentrations of DFBA ranging from 0 to 4 mM maintaining a BSA:DFBA ratios of 0:1, 1:10, 1:20, 1:30, 1:40, 1:60, 1:80, 1:100, 1:120, 1:160. A similar set of solutions is prepared for DFL–HSA maintaining 40:60 DMSO: H_2O solvent ratio. Further, 10 mM stock solutions of all the site markers (warfarin, tryptophan, naproxen and ibuprofen) except oleic acid are prepared in phosphate buffer (PB). The solution of oleic acid is prepared in DMSO. The final concentration of site markers in solution used for NMR measurements is kept at 2 mM. For STD experiments, solutions with 1:40 ratio of SA: test molecules are prepared. To confirm the effect of 40% DMSO on HSA structure, UV data are collected that confirmed no effect of 40:60 DMSO: H_2O solvent on the structure of HSA as shown in figure 3.2.

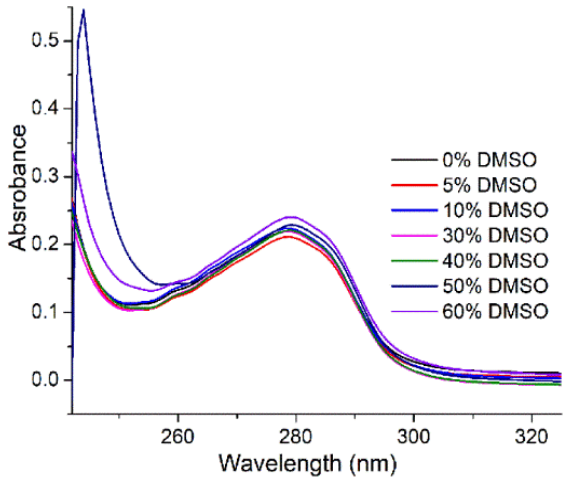

Figure 3.2: Effect of increasing (%) of DMSO in the aqueous buffer (pH=7.40) on the UV absorption spectra of HSA recorded at 298 K.

For part II, the stock solutions of 5 mM concentration of test molecules (DFL, DFBA, DFA) are prepared in DMSO-d_6 considering the solubility issues. The samples for NMR measurements contained 10 µM concentration of trypsin and a varying concentrations of test molecules (DFL, DFBA, and DFA) ranging from 0 to 1.6 mM maintaining a trypsin: test molecule ratios of 0:1, 1:30, 1:40, 1:50, 1:60, 1:80, 1:100, 1:120, and 1:160 similar to part I. A solvent composition of 25: 75 DMSO: aqueous PB has been maintained in all the above mentioned samples.

3.2.2 Details of NMR experiments:

All the NMR experiments are acquired on Bruker Ascend 500 MHz wide bore (WB) instrument. The temperature (T) has been maintained at 298 K throughout all experiments. 8 k (1 k=1024) data points (TD) are collected over a spectral width (SWH) of 12 ppm for all ^{19}F NMR experiments during the acquisition period while for ^{1}H NMR TD and SW of 16 k and 16 ppm respectively are used. 16 numbers of scans (ns) are used while recording all the NMR experiments. Relaxation delays of 5 s, 10 s and 12 s are used for DFL, DFBA and DFA in all NMR relaxation and diffusion experiments. ^{1}H NMR spectra are referenced with the residual water proton chemical shift. While in the absence of any reference ^{19}F compound, the ^{19}F NMR

spectra are reported in the Hz scale. The different NMR experiments performed are listed below.

1. ^{19}F T_1 measurements are performed using the standard spin inversion recovery (figure 2.9 (b), chapter 2) pulse sequence with ^{1}H decoupling for a total of 20 recovery periods ranging from 50 μs to 35 s.
2. ^{19}F T_2 are measured using CPMG pulse sequence with ^{1}H decoupling (figure 2.10 (b), chapter 2) for a total of 20 spin-echo repetitions varied from 2-8000 *i.e.* 8 ms to 32 s with a constant inter-pulse spacing (τ) of 2 ms.
3. Constant time relaxation dispersion CPMG (RD-CPMG) experiments are performed by varying the inter-pulse spacing between the π pulses (within the CPMG sequence figure 2.10 (b)) from 0.125 ms to 5 ms with a constant relaxation period of 50 ms. It is analogous to a spin locking technique where the locking field frequency (ν) and τ is related as $1/\tau = 2\nu$ [Dubois and Evers, 1992]. This method not only allows one to witness the exchange dynamics between ligand-protein but also quantifies the dissociation constant for the test molecule-SA complex.
4. For diffusion experiments using standard Bruker pulse sequence (figure 2.12, chapter 2), the gradient strength is varied linearly in 16 increments from 2 to 95% of the maximum gradient strength. The eddy current delay is kept as 5 ms for all the cases. Diffusion delay (Δ) of 100 ms, 50 ms and 50 ms are used for DFL, DFBA and DFBA respectively while diffusion gradient length (δ) are kept as 3 ms, 3 ms and 1.5 ms respectively.
5. For STD experiments (pulse sequence, figure 2.14 a & b in chapter 2), a Gaussian-shaped pulse of length 30 ms is used for selective excitation of protons at 0.75 ppm while the off-resonance excitation frequency is kept at 20 ppm. A total of 32 k TD are collected over a SWH of 50 ppm for both DFBA and DFL systems with a saturation time of 3 s and a spinlock period of 30 ms. 2048 scans are acquired with a d1 of 4 s in each case. ^{1}H–^{1}H STD with solvent presaturation is obtained by using Squa100.1000 shaped pulse of width 100 ms for solvent saturation.

3.3 RESULTS AND DISCUSSION:

3.3.1 Part-I: Interaction of Organofluorine with Serum Protein

(i) Chemical shift & Linewidth (FWHM): Determination of binding site. Figure 3.3 presents the proton decoupled ^{19}F NMR spectra of DFL (panel (i)) and DFBA (panel (ii)) in their free and bound form. Two distinct ^{19}F NMR signals appeared for DFL owing to the presence of two chemically distinct classes of fluorine while a sharp singlet is seen for DFBA due to chemical and magnetic equivalence of both the fluorine present at position 2 and 6 as shown in figure 3.3 (i a and ii a). As seen from figure 3.3 (i b & ii b), upon addition of 25 μM BSA, the ^{19}F spectral lines exhibited significant line broadening of *ca.* 8 Hz for DFL and ca. 3.6 Hz for DFBA along with the downfield shift of chemical shift positions on an average of 20 Hz for DFL and 8 Hz for DFBA respectively. This observation clearly indicates possible interactions between the test molecules and the protein. Since ligand-protein interaction is modeled as an equilibrium process between the ligand and the ligand-protein complex, the observed peak is actually a weighted average of the free and bound form of the ligand. Moreover, it also indicates existence of a fast exchange between the free and bound form of both the ligands on the ^{19}F NMR time scale resulting in a single peak [Zhuang, et al., 2013a]. Measurement and comparison of relaxation times of the ligand in the presence and absence of the protein confirmed the binding interaction between the ligands and SA. (The representative raw spectra and the resulting fitting curves through which values of T_1 and T_2 are determined is shown in figure 3.4 (I and II) respectively for the DFL-HSA system). These NMR observables are documented in table 3.1.

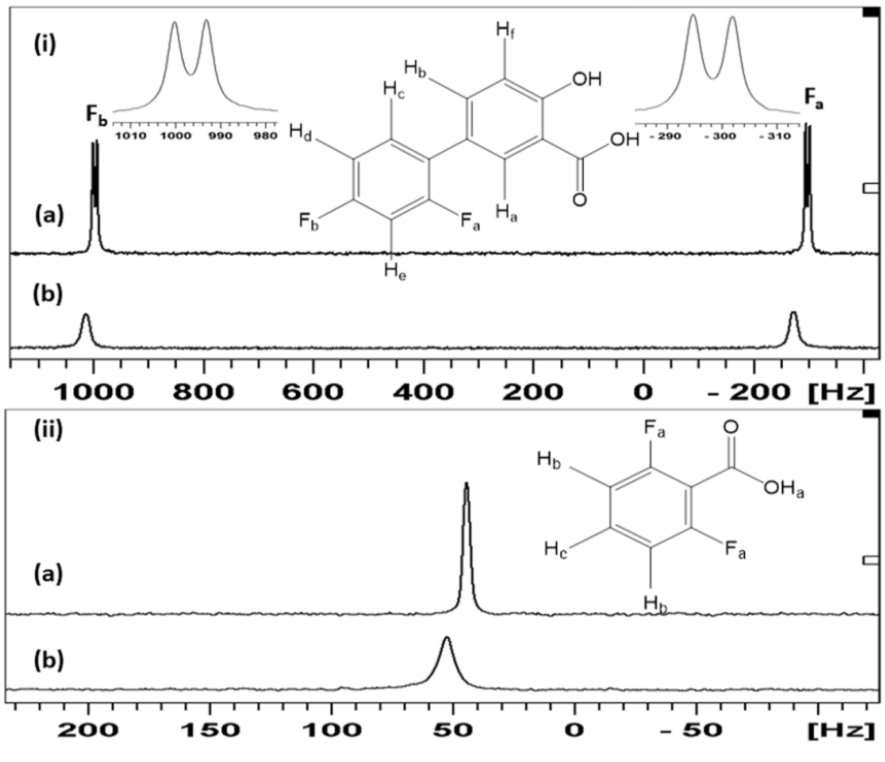

Figure 3.3: ^{19}F {^{1}H} NMR spectra and molecular structure of fluorine containing molecules under investigation (i) 1 mM DFL (ii) 1 mM DFBA (a) in the absence of SA and (b) in the presence of 25 µM SA. T= 298 K, pH=7.40.

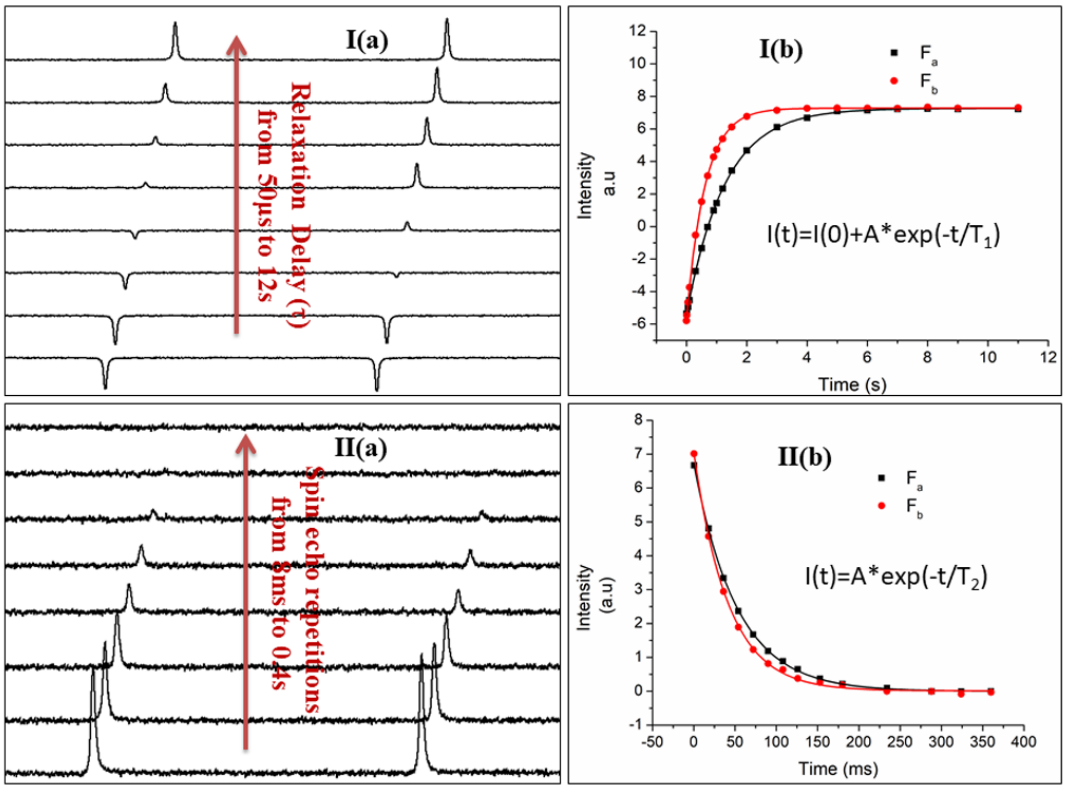

Figure 3.4: The representative raw spectra I (a) and II (a) and the resulting fitting curves I (b) and II (b) to determine T_1 (from inversion recovery experiment) and T_2 (from CPMG experiment) values respectively for DFL-HSA system. T= 298 K, pH=7.40.

Table 3.1 : NMR parameters for 2 mM DFL and 2 mM DFBA in the absence and presence of 25 µM SA recorded at T=298 K and pH=7.40

System	Chemical shift (Hz)	Linewidth (FWHM) (Hz)	T_1 (s)	T_2 (s)
DFL (F_a)	−297.71	10.74	0.682	0.552
(F_b)	996.29	10.93	1.374	1.088
DFL-HSA				
(F_a)	−272.81	17.95	0.598	0.023
(F_b)	1013.49	18.05	1.205	0.025
DFBA	44.21	3.22	2.302	2.212
DFBA–BSA	52.37	6.80	2.241	0.058

A close inspection of table 3.1 revealed that DFL experienced on an average 12% change in ^{19}F T_1 relaxation time going from free to bound state as compared to only 2.6% change observed for DFBA. Both the test molecules exhibit almost 97% change of T_2 values in the presence of SA. Comparisons of chemical shift, line broadening and spin-lattice relaxation time ascertain that overall change in NMR parameters in the presence of SA is to a greater extent in case of DFL compared to DFBA reflecting stronger binding of the former with SA. Subsequent to the preliminary confirmation of binding with SA, the determination of binding sites of these molecules on the protein is also undertaken. It is well known from literature that DFL binds to many sites on HSA, including sites I and II present in subdomain IIA and IIIA, respectively [Mao et al., 2001; Yang et al., 2013]. However, similar information regarding DFBA is not available as per our knowledge. Hence, a series of competition binding experiments are carried out in the case of DFBA–BSA. The four well-characterized site markers for serum albumins, *i.e.*, warfarin, ibuprofen, naproxen, and oleic acid, are used. Warfarin is known for its binding at the site I (subdomain IIA) [Kitamura et al., 2004] while ibuprofen binds at site II (subdomain IIIA) pockets of SA [Venturini et al., 2017]. On the other hand, oleic acid (the naturally occurring fatty acid), exhibits non-specific interaction with SA by binding to a number of sites in the protein with the highest binding affinity for domain III and subdomain IB. Naproxen however, binds at both site I and site II [Kitamura et al., 2004; Zhuang et al., 2013a, 2013b].

Figure 3.5 represents stack plots of $^{19}F\{^1H\}$ NMR spectra of competition binding experiments involving 1 mM DFBA in 50 µM BSA solution either in aqueous buffer or in 40:60 DMSO: aqueous buffer with different site markers as mentioned in figure legend. Figure 3.5 (a) and (b) in both the panels (I) and (II) exhibits the effect of the addition of protein to the free ligand solution. Figure 3.5 (c-e) in panel (I) displays the ^{19}F NMR stack plot of DFBA–BSA in aqueous buffer with warfarin, ibuprofen and, naproxen, respectively. In panel (II), figure 3.5 (f) represents a similar plot for oleic acid. The addition of warfarin and ibuprofen in DFBA–BSA solution resulted in an upfield shift of the peak towards free DFBA peak position along with the narrowing of the spectral line. This observation confirms that warfarin and ibuprofen are able to displace DFBA to bind at site I and site II in BSA. The addition of naproxen has also exhibited a similar effect. Even upon the addition of oleic acid, the signal tends to approach free DFBA chemical shift position that can be attributed to the non-specific binding of DFBA to BSA. The observed changes in ^{19}F chemical shift and linewidth of DFBA–BSA system are approximately similar on the addition of all the competing site markers with maximum changes occurring in the case of ibuprofen suggesting DFBA possessing a relatively higher binding affinity for site II. However, it will be more precise to state that the major binding of DBFA to BSA can be considered as non-specific where DFBA has multiple binding sites on BSA. The appearance of a

single ^{19}F signal for DFBA in the presence of the protein suggests that the molecule must be experiencing a fast exchange in its bound form between all the possible binding sites.

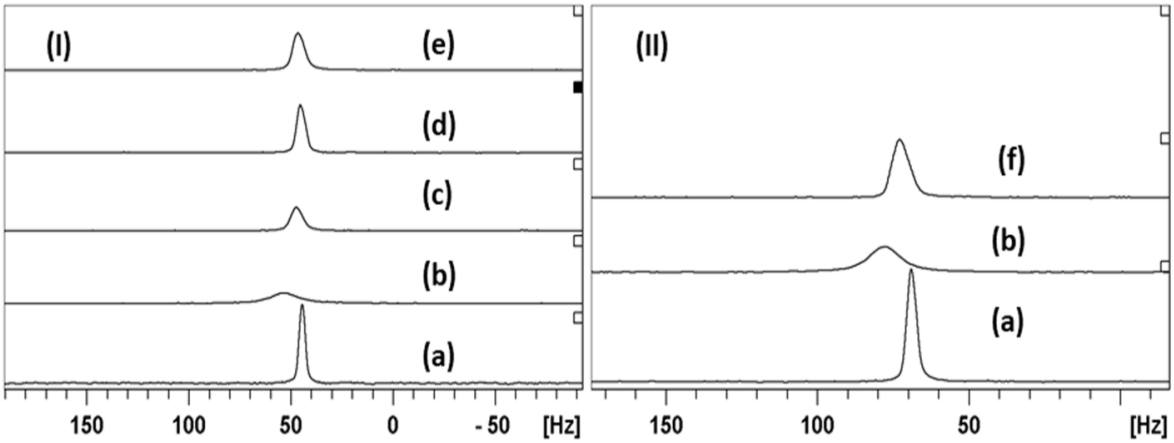

Figure 3.5: ^{19}F NMR spectrum of (I) (a) 1 mM DFBA (b) 1 mM DFBA-50 µM BSA in the absence of competing ligands (c) in presence of 1 mM warfarin (d) 1 mM ibuprofen (e) 1 mM naproxen in aqueous PB II) (a) 1 mM DFBA (b) 1 mM DFBA -50 µM BSA (f) 1 mM DFBA-50 µM BSA-1 mM oleic acid in 40:60 DMSO : aqueous PB.

(ii) Saturation Transfer Difference (STD): Confirmation of binding interaction.

$^{1}H–^{1}H$ STD and $^{19}F–^{1}H$ STD experiments are carried out for DFL–HSA, as shown in figure 3.6 (I) and 3.6 (II), respectively, following the procedure discussed in Chapter 2 (Section 2.6) [Mayer and Meyer, 1999]. The results matched well with the literature report [Sakuma et al., 2015]. The $^{1}H–^{1}H$ STD difference spectrum exhibited significant difference intensities for DFL protons that are in close proximity with the protein. The $^{19}F–^{1}H$ STD spectrum on integration revealed that the fluorine (F_b) at 1013.49 Hz is nearer to the binding site of HSA compared to the other fluorine (F_a) as it received significantly greater saturation. A similar set of $^{1}H–^{1}H$ STD and $^{19}F–^{1}H$ STD experiments are carried out for DFBA–BSA system as shown in figure 3.7 (I) and 3.7 (II) respectively. For both the molecules, the difference spectrum (c) has been intensified/ scaled up by 32 times for visible representation.

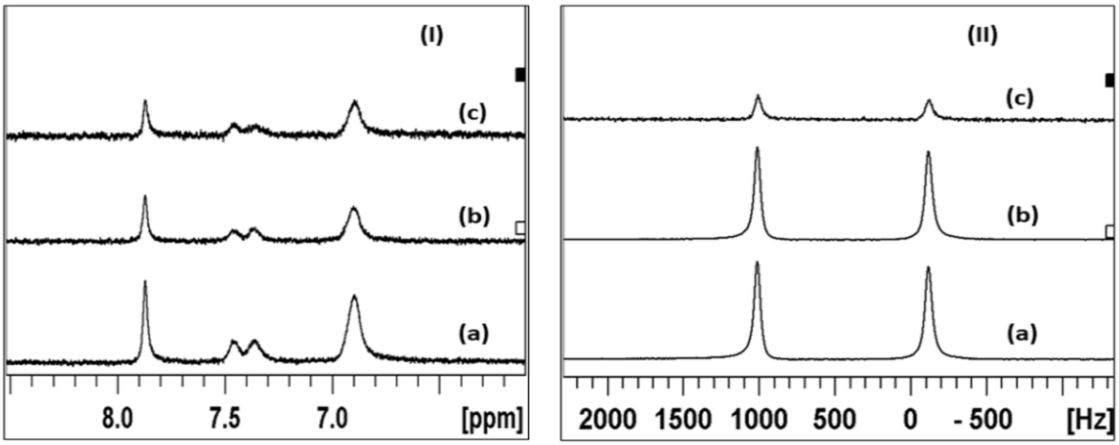

Figure 3.6: (I) (a) ^{1}H spectrum (STD_{off} resonance) and (b) ^{1}H STD_{on} resonance spectrum (c) ^{1}H STD difference spectrum of 0.050 mM HSA and 2.0 mM DFL. (II) (a) ^{19}F spectrum (STD_{off} resonance) and (b) ^{19}F $\{^{1}H\}$ STD_{on} resonance spectrum (c) ^{19}F STD difference spectrum of 0.050 mM HSA and 2.0 mM DFL . T=298 K, pH= 7.40.

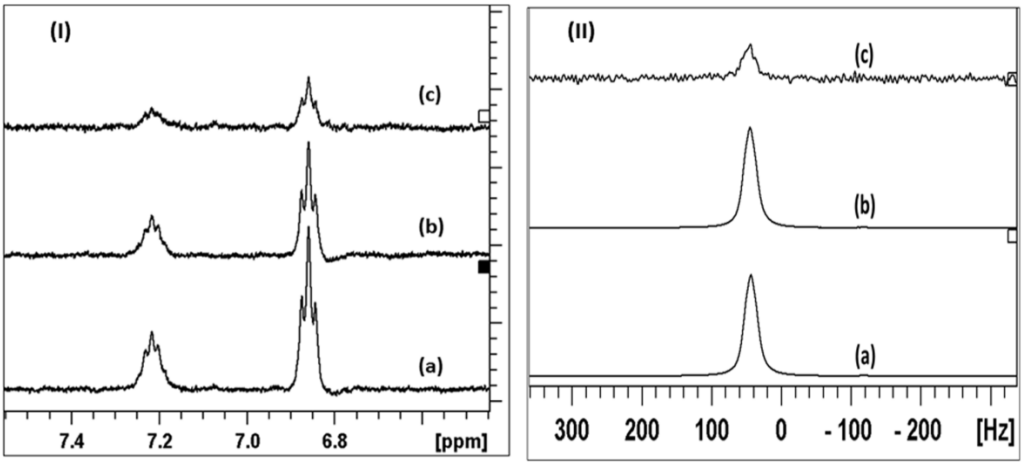

Figure 3.7: (I) (a) ^{1}H spectrum (STD_{off} resonance) and (b) ^{1}H STD_{on} resonance spectrum (c) ^{1}H STD difference spectrum of 0.050 mM BSA and 2.0 mM DFBA. (II) (a) ^{19}F spectrum (STD_{off} resonance) and (b) ^{19}F $\{^{1}H\}$ STD_{on} resonance spectrum (c) ^{19}F STD difference spectrum of 0.050 mM BSA and 2.0 mM DFBA. T= 298 K, pH=7.40.

Figure 3.7 (I) clearly exhibits that DFBA proton H_c experienced greater saturation than proton H_b indicating that H_c of DFBA is proximal to the binding site of BSA compared to H_b. Also, significant difference intensity is observed in case of ^{19}F–^{1}H STD difference spectrum of DFBA that provides further evidences of the interaction between DFBA and BSA. In both the cases it can be predicted that binding of test molecules preferentially occurs through the aromatic ring side while the non-fluorinated functional groups (–COOH) remained oriented away from the binding site of SA.

(iii) Diffusion and spin-spin relaxation time (T_2): Determination of dissociation constant (K_D) & number of binding sites (n):

Ligand NMR parameters measured in the presence of protein is, in reality, a weighted average of two different ligand environments, *i.e.,* free state and the bound state of the ligand. In case the ligand exchanges very fast between these two states giving rise to single coalesced peak for ligand resonances, the measured relaxation and diffusion parameters will reflect the effect of chemical exchange. Hence it is advisable to use NMR pulse sequences that will allow the determination of accurate and realistic NMR parameters [Dubois and Evers, 1992; Lucas and Larive, 2004]. On the other hand, judicious choices of experimental parameters will facilitate the extraction of the exchange rate and lifetime of the bound state.

A point to be mentioned here that chemical shift, relaxation time (T_1 & T_2), and diffusion coefficient have also been measured for series of ligand concentration (0.5 mM to 4 mM in absence of protein) as control. These parameters do not depict any significant change in their values as a function of ligand concentration in the absence of protein. This observation rules out any possibility of aggregation. A representative plot of these NMR parameters for DFBA as a function of series of concentration of free ligand has been shown in Annexure A as figure A1.

Diffusion coefficient measurements and analysis: In the present case, the BPPLED pulse sequence shown in figure 2.12 (chapter 2, section 2.5) has been employed where a series of spectra are acquired with increasing gradient strength and keeping Δ and δ values constant [Price et al., 2002]. The representative raw spectra and the resulting fitting curves through which values of D are determined are shown in figure 3.8 (I and II) for both the DFL–HSA & DFBA–BSA system respectively. Table 3.2 documents the experimentally determined D values for DFL and DFBA is absence and presence of SA.

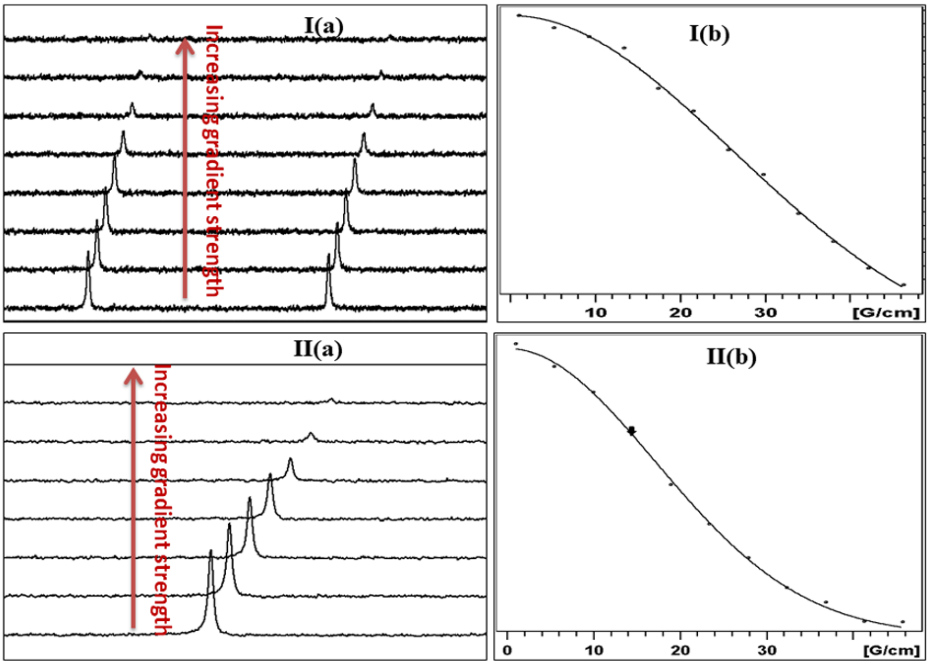

Figure 3.8: The representative raw spectra I (a) and II (a) and the resulting fitting curves I (b) and II (b) to determine *D* value for (I) DFL–HSA and for (II) DFBA–BSA system. Equation 2.20 is used to fit these plots.

Table 3.2: Representative experimentally measured diffusion coefficient (D) and relaxation rate (R_2) data for ligands in absence and presence of SA used for plotting figure 3.10 and 3.11 (presented later). T= 298 K, pH=7.40

Protien: Ligand	**DFL:HSA**			**DFBA:BSA**	
(mM)	$D\times10^{-10}$ (m^2/s)	R_2 (s^{-1}) (F_a)	R_2 (s^{-1}) (F_b)	$D\times10^{-10}$ (m^2/s)	R_2 (s^{-1})
0:1	2.730	1.811	0.911	7.480	0.429
0.025:0.5	1.911	60.382	65.750	6.513	24.715
0.025:0.75	–	–	–	6.678	21.733
0.025:1	2.107	51.667	48.0433	6.750	19.232
0.025:1.5	2.257	40.296	37.041	6.869	16.394
0.025:2	2.309	34.048	31.78	6.995	13.69
0.025:2.5	2.389	27.801	27.613	7.059	11.904
0.025:3	2.440	24.677	22.901	7.117	10.101
0.025:4	2.507	20.011	17.097	7.189	8.330

As mentioned before, under fast exchange conditions, the observed diffusion coefficient is a weighted average value of the ligand diffusion coefficients in its free and bound state, as given by equation 2.21 (chapter 2, section 2.5). P_b, the bound ligand population in equation 2.21 can be further written as equation 3.1:

$$P_b = \alpha - \sqrt{\alpha^2 - \beta} \quad \text{.....(3.1)}$$

where,

$$\alpha = \frac{C_L + nC_P + K_D}{2C_L} \qquad ; \qquad \beta = \frac{nC_P}{C_L}$$

n: number of binding sites, C_L: Ligand concentration, C_P: Protein concentration, K_D: Dissociation constant.

At this juncture, it must be noted here that fluorescence competition binding experiments for DFL reported in the literature [Yang et al., 2013] and the competition binding experiments performed for DFBA–BSA system that has been discussed in section 3.3.1 (i) indicated multiple binding sites. Hence, before extracting the dissociation constants for the test molecules-SA complexes considering two site exchange model, it is meaningful to establish the concept of cooperativity among the different binding sites available on SA. Cooperativity in present case for macromolecules (*i.e.* SA), having two or more binding sites is described as the change in the equilibrium binding affinity of a ligand towards a given binding site by the occupancy of other sites by the same or different ligands [Cattoni et al., 2015]. Simply, the binding of ligand on one of the macromolecule site activates or deactivates the other binding sites in the same molecule. To examine the cooperativity amongst the multiple binding sites of SA for test molecules, the Hills and Scatchard plots (figure 3.9) are generated using the protein-bound fraction. Equation 3.2 is known as the Hill equation, where n_H (Hills coefficient) determines whether cooperativity exists or not amongst the multiple binding sites present on the protein for a particular ligand. A word of caution to note that n_H should not be confused with the number of binding sites (n).

$$\log \frac{Y}{1-Y} = n_H \log L_{free} - \log K_D \text{.....(3.2)}$$

where Y =fractional saturation of protein *i.e.,* bound protein fraction and is given as:

$$Y = \frac{[PL]}{n[P_t]} = \frac{L_{free}}{K_D + L_{free}} \text{.....(3.3)}$$

Here, L_{free} stands for free ligand concentration present in solution; [PL] is the concentration of bound ligand complex; P_t represents the total protein concentration, and K_D is the dissociation constant. As per literature reports for different values of n_H, obtained from plot of log$(Y/1-Y)$ vs. log (L_{free}) the following conclusions can be drawn:

(a) Slope n_H =1 indicates existence of non-cooperative binding in case of multiple binding sites confirming that all the binding sites are identical and equivalent.

(b) For n_H >1 the binding shows positive cooperativity.

(c) For the highly cooperative binding, n_H can be approximated to the number of binding sites n.

(d) For n_H <1, negative cooperativity exists.

Similar information can be obtained by using equation 3.4 popularly known as the Scatchard equation and is given as:

$$\frac{Y}{L_{free}} = \frac{n}{K_D} - \frac{Y}{K_D} \text{.....(3.4)}$$

Deviation from linear Scatchard plot (Y/L_{free} vs. Y) indicates the presence of cooperativity. A concave upward behaviour in place of a linear plot is a measure of negative cooperativity while concave downward behaviour from linearity represents positive cooperativity.

The linear behavior of both the plots (figure 3.9 a & b) confirms in the present case, the absence of any type of cooperativity amongst the binding events [Byers, 1977; Rippe, 1997; Sabouri and Movahedi, 1994; Sears et al., 2007; Stefan and Novère, 2013; Wilhelms and Normant, 1985]. The relevant parameters are tabulated in table 3.3.

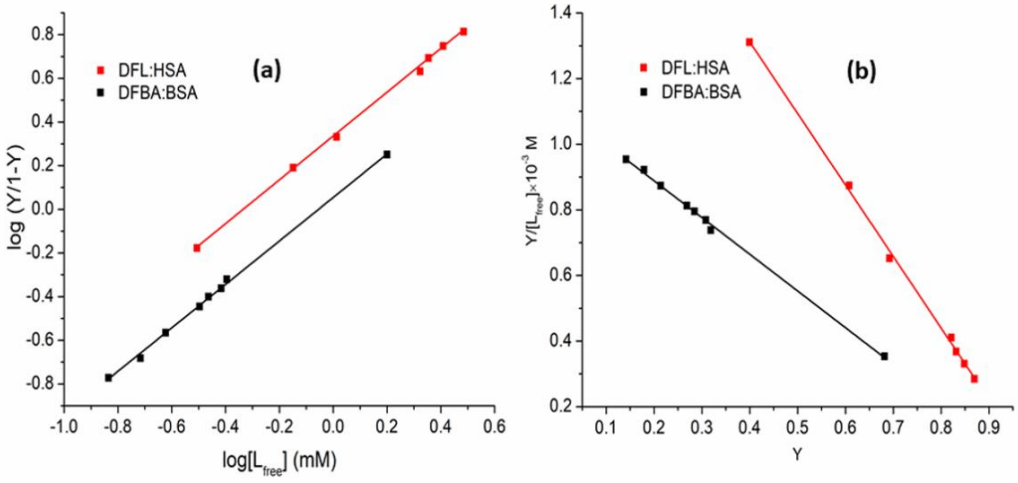

Figure 3.9: (a) Hills Plot and (b) Scatchard Plot for binding of DFL: HSA and DFBA: BSA system. Symbols represent the experimental data while solid lines represent the linear fit to the data. T= 298 K, pH=7.40.

Table 3.3: Relevant parameters *i.e.*, dissociation constant (K_D) and slope obtained from (a) Hills Plot (b) Scatchard Plot. T= 298 K, pH=7.40.

System	Hills Plot			Scatchard Plot	
	K_D (mM) (from intercept)	Slope (n_H)	R^2	K_D (mM) (from intercept)	R^2
DFL:HSA	0.461±0.101	0.996	0.998	0.457 ±0.116	0.997
DFBA:BSA	0.879 ±0.123	1.003	0.999	0.900±0.142	0.998

Therefore, this can be rationalized by stating that all the binding sites on SA are independent of each other and will exhibit an equal binding affinity towards the test ligands. Hence, in the present case, we have considered the simple model that assumes that both DFL and DFBA exhibit an equal binding affinity for all the sites on SA. The equations 2.21 and 3.1 are, therefore, valid for determining single macroscopic dissociation constant for DFL–HSA and DFBA–BSA complexes respectively [Liu et al., 1997; Luo et al., 1999].

Figure 3.10 (a & b) represents the plot of experimentally measured ^{19}F diffusion coefficients with increasing ligands concentrations using the data given in table 3.2. A non-linear least-square fitting of the experimental data employing the equation 3.1 is adopted using MATLAB software to derive the ligand-protein dissociation constant (K_D) and the number of binding sites (n). It must be noted here that a single dissociation constant has been extracted for both the ligands as discussed above and reported latter in table 3.4. The value of diffusion coefficient for pure protein SA is taken to be 0.64×10^{-10} m^2/s as per literature [Price et al., 2002] while for free DFL & DFBA, the diffusion coefficients are evaluated to be 2.73×10^{-10} m^2/s and 7.48×10^{-10} m^2/s respectively.

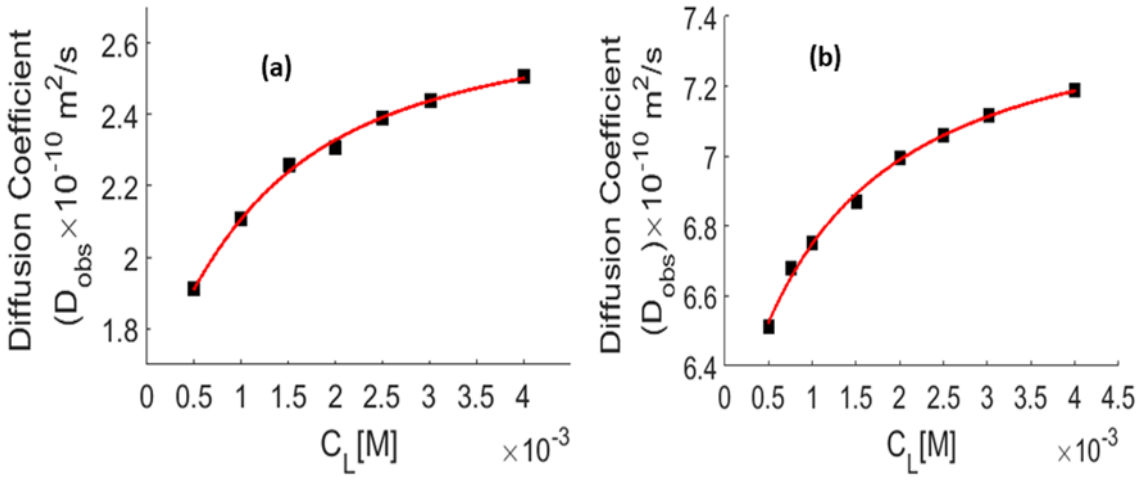

Figure 3.10: Plot of the observed diffusion coefficient versus the concentration of (a) DFL (b) DFBA for the DFL: HSA and DFBA: BSA system, respectively. BSA=25 µM. Symbols represent the experimental data. The solid line represents the fitting of experimental data. T= 298 K, pH=7.40.

^{19}F transverse relaxation rate measurements: Measurement of transverse relaxation rates (R_2) employing the CPMG pulse sequence and using the smallest inter-pulse spacing *ca.* τ = 0.125 ms can also readily identify the ligand-protein binding event. At such a small interpulse spacing, the contribution of ligand exchange between free and the bound state is minimized [Dubois and Evers, 1992]. Hence, the experimentally determined R_2 values would give rise to a realistic estimation of K_D and n. Figure 3.11 (a & b) displays the plot of ^{19}F R_2 measured for DFL and DFBA in the presence of 25 µM SA with increasing ligand concentrations. Equations 2.21 and 3.1 are equally valid to fit relaxation data by replacing D with R_2 ($1/T_2$) in case of a fast exchange limit [Stockman and Dalvit, 2002]. Since both the ligands are exhibiting fast exchange in the presence of SA, we adopted the determination of K_D and n from the relaxation data as well by employing equations 2.21 and 3.1. The experimentally measured relaxation rates used to plot figure 3.11 have been given in table 3.2.

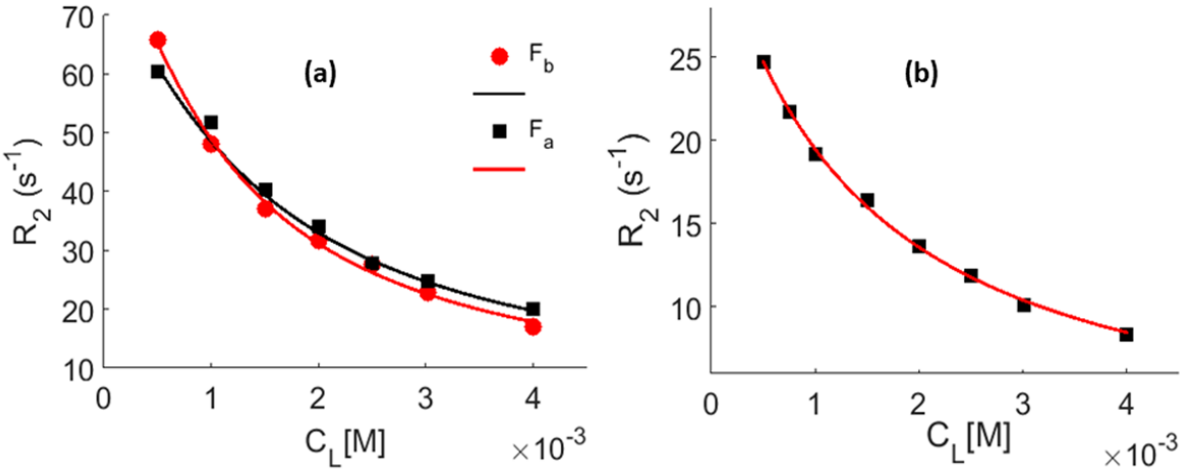

Figure 3.11: Plot of the observed transverse relaxation time versus the concentration of (a) DFL (F_a) & DFL (F_b) for the DFL: HSA system (b) DFBA for DFBA: BSA system. BSA=25 µM. Symbols represent the experimental data. The solid line represents the fitting of experimental data. T= 298 K, pH=7.40.

Parameters like chemical shift and relaxation times (T_1, T_2) for a ligand generally alter on binding to protein [Fielding, 2007]. However, these values for the fully bound state of the ligand are obtained only by extrapolating the graph of chemical shift/relaxation vs. concentration plot. Consequently, K_D and n extracted from such extrapolated data could be completely unrealistic. As a remedy one may try to determine say for example, the relaxation time of the bound ligand by fitting the data using the K_D and n values obtained from diffusion analysis [Liu et al., 1997]. In table 3.4, the values of K_D and n obtained from diffusion as well as relaxation data have been documented for the purpose of comparison. In the case of DFL, both K_D and n determined by diffusion and relaxation are within 10% of each other while in case of DFBA deviation in these values determined by diffusion and relaxation are on a higher side. Furthermore, the bound ligand fractions are also calculated using equation 2.21 for the entire set of samples and are reported in table 3.5. From table 3.5, it is found that for same ratio of protein: ligand, P_b value for DFL is nearly 2.7 times greater than that for DFBA. Also, DFL has a greater number of binding sites to SA than DFBA. The number of binding sites of a molecule to SA can in principle, characterize the binding capacity of that molecule [Luo et al., 1999].

Table 3.4: Dissociation constant (K_D) and the number of binding sites (n) obtained from relaxation and diffusion measurements. T= 298 K, pH=7.40.

Systems	Diffusion		Relaxation	
	K_D (mM)	n	K_D (mM)	n
DFL–HSA	0.458±0.19	20±2	0.394±0.11 (F_a) 0.589±0.09 (F_b)	19±2 22±4
DFBA–BSA	0.8676±0.22	8±1	1.0043±0.15	10±1

Table 3.5: Bound ligand fraction (P_b) obtained from relaxation and diffusion measurements. T= 298 K, pH=7.40.

Protein: Ligand	DFL:HSA		DFBA:BSA	
(mM)	P_b (%) calculated from diffusion data	P_b (%) calculated from Relaxation data (average value)	P_b (%) calculated from diffusion data	P_b (%) calculated from relaxation data
0.025:0.5	39.95	40.13	14.16	14.56
0.025:0.75	–	–	11.60	12.78
0.025:1	30.39	30.86	10.69	11.31
0.025:1.5	23.07	24.10	8.95	9.64
0.025:2	20.53	20.08	7.11	8.05
0.025:2.5	16.63	17.01	6.16	7.00
0.025:3	14.14	14.27	5.31	5.94
0.025:4	10.87	11.21	4.26	4.90

Further, competition binding experiments are also performed to confirm the binding ability of DFL compared to that of DFBA. Figure 3.12 represents the same and reiterates that DFL is a stronger binder to SA than DFBA. Figure 3.12 shows stack plot of DFL added to DFBA–HSA. Addition of DFL replaces DFBA from the complex as can be seen from chemical shift and line width of DFBA becoming closer to the values of free DFBA. Similarly, figure 3.12 (b) represents stack plot of DFL–HSA solution after addition of DFBA. Addition of DFBA is not able to induce

any change in chemical shift and linewidth of DFL in presence of HSA. Therefore, values of n along with K_D and the results of competition binding experiments suggest that DFL is a better binder to SA than DFBA. These values of n and K_D also confirm for non-specific nature of binding of the test ligands to SA.

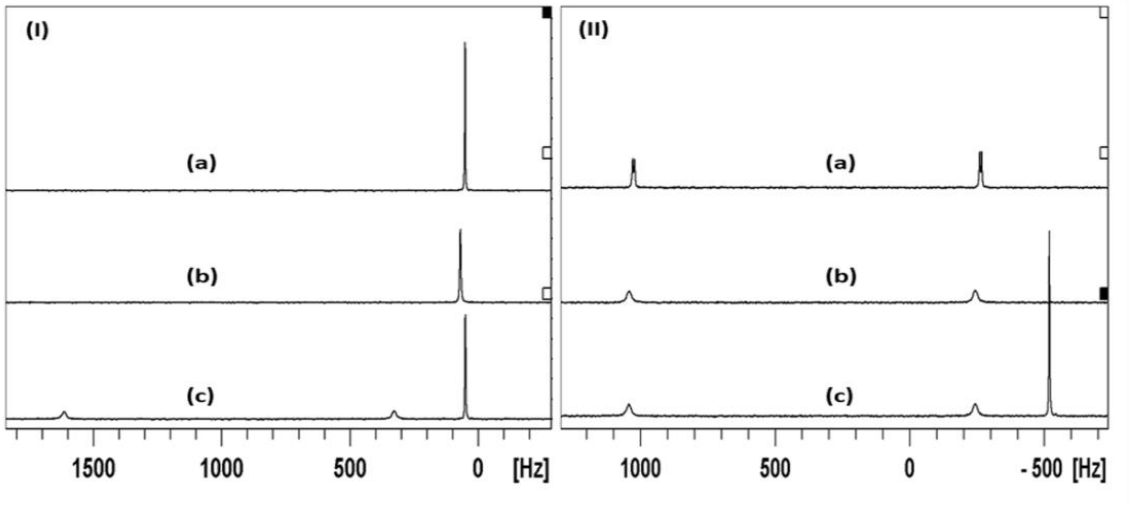

Figure 3.12: ^{19}F NMR spectrum of (I) 2 Mm DFBA (a) 2 mM DFBA in presence of 25 µM HSA (b) 2 mM DFL added in 2 mM DFBA–25 µM HSA (c) (II) 2 mM DFL (a) 2 Mm DFL in presence of 25 µM HSA (b) 2 mM DFBA added in DFL –25 µM HSA (c) in 40:60 DMSO : aqueous buffer solvent. T= 298 K, pH=7.40.

In the following section, the effect of chemical exchange on relaxation rate and further the extraction of the exchange rates have been addressed by employing RD-CPMG experiments for both DFL–HSA and DFBA–BSA complexes.

(iv) Constant time fast pulsing CPMG: Extraction of exchange rate, residence time.

One may attempt to quantify the chemical exchange process existing between the free and the bound state of the ligand in the presence of the protein. In literature, there are a few examples where researchers have employed constant time fast pulsing CPMG experiment to achieve the same [Dubois and Evers, 1992; Gerig and Stock, 1975; Xu et al., 1996]. This experiment is very similar in principle with the relaxation dispersion (RD) CPMG experiments employed for quantifying macromolecular dynamics in solution. It has become a powerful technique to quantify the exchange process in the microsecond to millisecond regime (intermediate to fast exchange) [Millet et al., 2000; Mittag et al., 2003]. Though, there are number of pulse sequences reported for characterizing dynamics of proteins, [Kleckner and Foster, 2010; Kovrigin et al., 2006; Millet et al., 2000] a handful of reports are available on ligand detected relaxation dispersion experiments to quantify ligand-protein binding [Lin, 2016; Moschen et al., 2015, 2016]. In the present study, ligand observed ^{19}F fast pulsing CPMG sequence is employed following Dubois *et al.* [Dubois and Evers, 1992]. In fast pulsing CPMG measurements, the magnitude of R_2 is heavily influenced by the rate of exchange between free ligand and the ligand-protein complex and therefore appeared as a population-averaged value of the free and the bound states of the ligand. Hence, the approach is to observe and quantify exchange kinetics by probing the variation in R_2 (the result of chemical exchange that leads to broadened linewidth) as a function of inter-pulse spacing (τ) between the π pulses used in the CPMG sequence. In other words, exchange broadening is nullified by using series of spin-echo pulse elements (τ-180-τ) with a τ period that is small enough to avoid the effect of exchange.

The two-site exchange kinetic model [Kovrigin et al., 2006] of ligand (L) binding to protein (P) (L+P ↔ LP) is applied to quantify exchange rate by plotting the dependence of measured relaxation rate (R_2) on inter-pulse spacing (τ). In constant time CPMG, R_2 is monitored as a function of ν_{cpmg} at which π pulses are applied with a constant transverse relaxation time of T_{relax}. Equation 3.5 represent the simpler form of the general equation given by Carvers & Richards [Carver and Richards, 1972] for R_2 as a function of τ in case of a two site exchange process with $K_{ex} >> \Delta\omega$ (fast exchange), and can be written as [Kleckner and Foster, 2010; Millet et al., 2000]:

$$R_2(1/\tau) = R_2^0 . + \phi_{ex} / K_{ex}(1 - \frac{2\tanh(K_{ex}\tau/2)}{(K_{ex}\tau)}) \text{.....(3.5)}$$

Further, equation 3.5 can be rewritten as equation 3.6 by expressing the inter-pulse spacing in terms of ν_{cpmg}.

$$R_2 = R_2^0 + \frac{\phi_{ex}}{K_{ex}}\left(1 - \frac{4\nu_{cpmg}}{K_{ex}}\tanh\left(\frac{K_{ex}}{4\nu_{cpmg}}\right)\right) \text{.....(3.6)}$$

here,

$$\nu_{cpmg} = 1/4\tau_{cpmg}$$

In equations 3.5 and 3.6, $2\tau_{cpmg}=\tau$ is the time between successive refocusing pulses, K_{ex} is the apparent exchange rate, R_2^0 is the magnitude of relaxation rate at $\nu_{cpmg}= \infty$ and can be estimated by extrapolating the plot of R_2 vs. ν_{cpmg}. Equation 3.7 represents ϕ_{ex} in terms of populations of both sites and the chemical shift difference.

$$\phi_{ex} = P_a P_b \Delta\omega^2 \text{.....(3.7)}$$

where,

$$P_a + P_b = 1,$$

$$\Delta\omega = 2\pi\Delta\delta B_0$$

P_a and P_b represent the fractional population of the ligand in free and bound state. $\Delta\delta$ = chemical shift difference between free and completely bound ligand form. B_0 is the magnetic field strength at which experiments are carried out. Although $K_{ex,}$ as given in equation 3.5 and 3.6, is informative, exchange kinetics is more efficiently described by individual forward and reverse rate constants.

Hence, the apparent exchange rate can be rewritten as given in equation 3.8:

$$K_{ex} = K_{on} \times [P] + K_{off} \text{.....(3.8)}$$

where, [P] denotes the concentration of free protein. K_{on} and K_{off} are the association and dissociation rate constants, respectively, of the complex. It is challenging to extract the values of P_a, P_b, and $\Delta\omega$ as depicted in equation 3.7 [Kleckner and Foster, 2010]. However, an estimate of P_b and P_a can be obtained using equations 3.9 and 3.10.

$$P_b = P_{bound} = K_{on} \times [P] / (K_{on} \times [P] + K_{off}) \text{.....(3.9)}$$

$$P_a = K_{off} / (K_{on} \times [P] + K_{off}) \text{.....(3.10)}$$

Figure 3.13 (a and b) displays the RD profiles for samples with varying SA: test molecule ratio at following CPMG field strengths: 50, 100, 125, 200, 250, 300, 400, 550, 650, 1000, 1250, 1666.6 and, 2000 Hz. The values of R_2 measured at corresponding field strength for two concentrations have been tabulated in representative table 3.6.

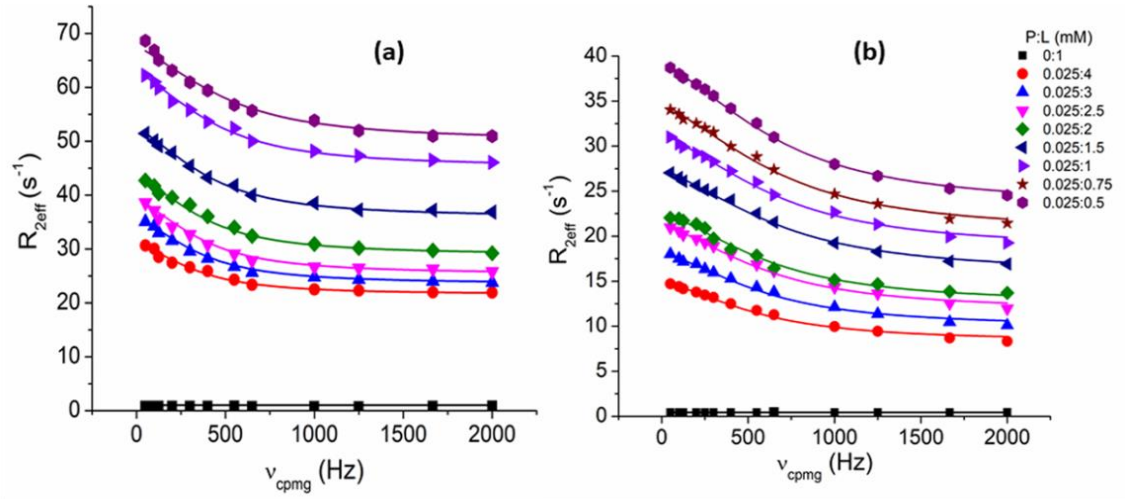

Figure 3.13: Relaxation dispersion ^{19}F profiles obtained at 500 MHz for (a) DFL (b) DFBA in the absence and presence of SA. A flat relaxation dispersion profile is observed for free DFL and DFBA. In the presence of SA, the dispersion profiles display a significant dependence on the concentration of ligand: protein ratio. Symbols represent experimental data with solid lines representing two-state numerical fits. T= 298 K, pH=7.40.

Table 3.6: Representative data showing the change in relaxation rate (R_2) of DFL and DFBA in DFL: HSA and DFBA:BSA system with field strength as plotted in figure 3.13 at T= 298 K and pH=7.40.

υ_{cpmg}	R_2 (s^{-1}) values for DFL:HSA		R_2 (s^{-1}) values for DFBA:BSA	
(Hz)	4:0.025 mM	1:0.025 mM	4:0.025 mM	1:0.025 mM
2000	21.935	46.063	8.333	19.274
1666.66	21.972	46.499	8.688	19.933
1250	22.265	47.305	9.432	21.321
1000	22.491	48.177	9.962	22.665
650	23.366	50.012	11.264	24.593
550	24.309	52.426	11.76	26.001
400	25.891	53.63	12.492	27.235
300	26.591	55.823	13.199	28.273
200	27.438	57.369	13.787	29.232
125	28.517	59.835	14.156	29.898
100	30.050	61.003	14.390	30.251
50	30.632	62.23	14.695	31.006

In figure 3.13 (a & b), a flat RD profile (negative control) is observed for free DFL and DFBA, indicating the absence of any chemical exchange contribution as well as any interference in the experiment due to residual couplings causing variation in R_2 [Moschen et al., 2016]. On the other hand, the addition of SA to the free test molecules induces changes in relaxation rates due to chemical exchange between the free and bound state of the ligand resulting in a non-flat dispersion profile. Such a non-flat dispersion profile, therefore, also confirms the interaction between test molecules and SA. Subsequently, these profiles are fitted simultaneously using Microcal Origin Pro 9.0 plotting software using equation 3.6 (K_{ex} can be split in terms of K_{off} and K_{on} according to equation 3.8) giving global K_{off} and corresponding $K_{on} \times [P]$ value for each concentration ratio as shown in table 3.7.

Table 3.7: Summary of data obtained from non-flat dispersion profiles (CPMG) for ligands in presence of SA**.**

Concentration (P:L) mM	DFL:HSA			DFBA:BSA		
	P_b (%)	$K_{on} \times [P]$ (s^{-1})	K_{off} (s^{-1})	P_b (%)	$K_{on} \times [P]$ (s^{-1})	K_{off} (s^{-1})
0.025:4	10.86±1.44	250±38	2050 ±90	4.45±1.91	210±86	4500 ±160
0.025:3	14.86±1.94	358±56		5.30±2.04	252±99	
0.025:2.5	17.17±2.33	425±72		6.35±2.31	306±125	
0.025:2	19.9±2.88	512±93		7.36±2.47	358±137	
0.025:1.5	24.24±2.53	656±105		8.59±3.03	423±169	
0.025:1	29.93±2.67	880±113		10.21±3.25	512±188	
0.025:0.75	–	–		12.24±3.22	628±195	
0.025:0.5	38.70±2.29	1294±131		13.61±3.34	709±210	

In table 3.7, the results obtained from numerical fitting of two-site exchange model for non-flat dispersion profiles providing a single K_{off} for various SA: ligand ratio along with the respective values of $K_{on} \times [P]$ has been reported. The average exchange rate (K_{ex}) determined from the K_{off} and average of K_{on} values as reported in table 3.7 are 2670±120 s^{-1} in the case of DFL and 4920±200 s^{-1} in case of DFBA. K_{ex} obtained is closer to the value of K_{off} as expected for the fast exchanging system in both the cases. The bound fraction is calculated using equation 3.9, and the values obtained match well with those determined from the diffusion experiments. The values tabulated in table 3.7 exhibit a decrease in bound fraction with the increase of concentration of protein: ligand from 0.025:0.5 mM to 0.025:4 mM. The constant time CPMG experiments are repeated at least twice in both the cases of DFL and DFBA to figure out the uncertainties of K_{off} resulting from the inseparable term ϕ_{ex}. The K_{ex} values determined from the repeat experiments are reported with standard deviation. The residence time of a ligand, as defined by $\tau_{res} = 1/K_{off}$ has been calculated and found to be 0.49 ms and 0.22 ms for DFL: HSA and DFBA: BSA, respectively. The residence time (lifetime of the complex) strongly depends on the nature of the interactions between ligand and protein and indicates the duration for which the ligand will remain bound to the target that governs the activity of the ligand [Copeland, 2016; Moschen et al., 2016]. A longer residence time determined for DFL: HSA confirms DFL as a better binder to SA.

3.3.2 Part-II: Organofluorine with Trypsin

(i) Chemical shift and line-broadening:

Figure 3.14 (a, b, c) represents the ^{1}H decoupled ^{19}F NMR spectrum of 1 mM test molecules namely DFL, DFBA, and, DFA respectively in absence and presence of 10 μM trypsin. ^{1}H decoupling ensures the sensitivity improvement for the fluorine signal in the ^{19}F NMR spectrum as fluorine is usually scalar coupled with several protons [Dalvit et al., 2003]. ^{19}F NMR spectra of DFA showed a single ^{19}F resonance as it consists of a single type of fluorine nuclei. The spectra of test molecules in the presence of trypsin do not exhibit any significant change in chemical shift and line-broadening with the addition of trypsin. Further, the ^{1}H NMR spectra of the test molecules as a function of trypsin concentration are also acquired to comment on the interaction of test molecules with trypsin. ^{1}H NMR spectra of DFL, DFBA, and DFA again do not reveal any visible change in chemical shift and line-broadening with the addition of trypsin. This observation accounts for either the absence of any molecular interaction or the presence of extremely weak non-covalent interaction of these molecules with trypsin that is beyond detection.

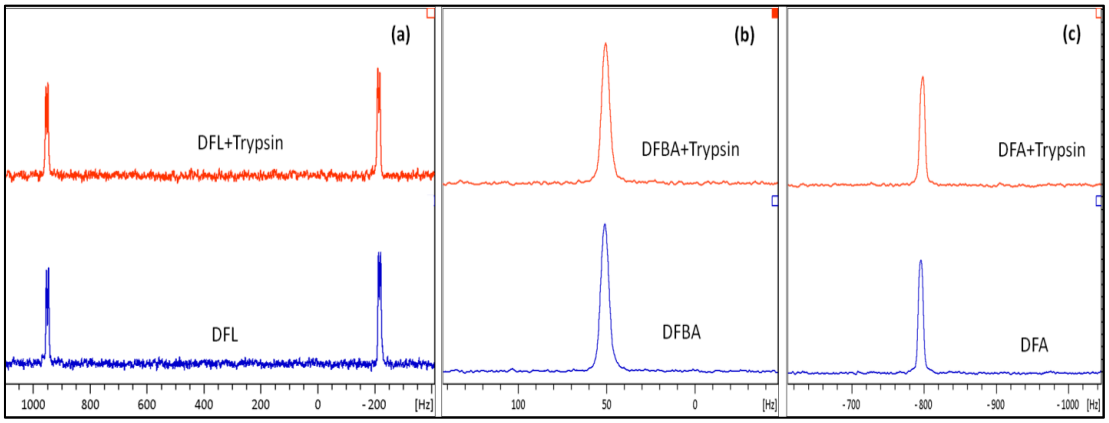

Figure 3.14: ^{1}H decoupled ^{19}F NMR spectrum of 1 mM (a) DFL (b) DFBA and (c) DFA in the absence and presence of 10 μM trypsin recorded at 298 K and pH=7.40.

An attempt to record the ^{1}H–^{1}H and ^{19}F–^{1}H STD difference spectra for test molecules-trypsin did not result in any peak of significant intensity ruling out the possibility of any weak interaction between these fluorochemicals and trypsin (data not shown). However, we proceed with quantitative analysis of ligand-protein binding through measurement of ^{19}F transverse relaxation rates and self-diffusion constants. These measurements further strengthen the evidence of ligand binding obtained from 1D NMR measurements.

(ii) Relaxation and Diffusion:

R_2 and D values of DFL, DFBA and, DFA in the presence of trypsin are determined and plotted as function of ligand concentration (C_L) as shown in figure 3.15. It is well known that the chemical shift changes and line-broadening are generally of smaller magnitude and do not show any significant changes if non-covalent interaction occurs. Also, false signals in the STD difference spectrum can appear if all the STD parameters are not well optimized or if there are strong binding interaction between ligand and protein. Therefore, the relaxation and diffusion plots shown in figure 3.15 are the ultimate signature of ligand-trypsin interaction.

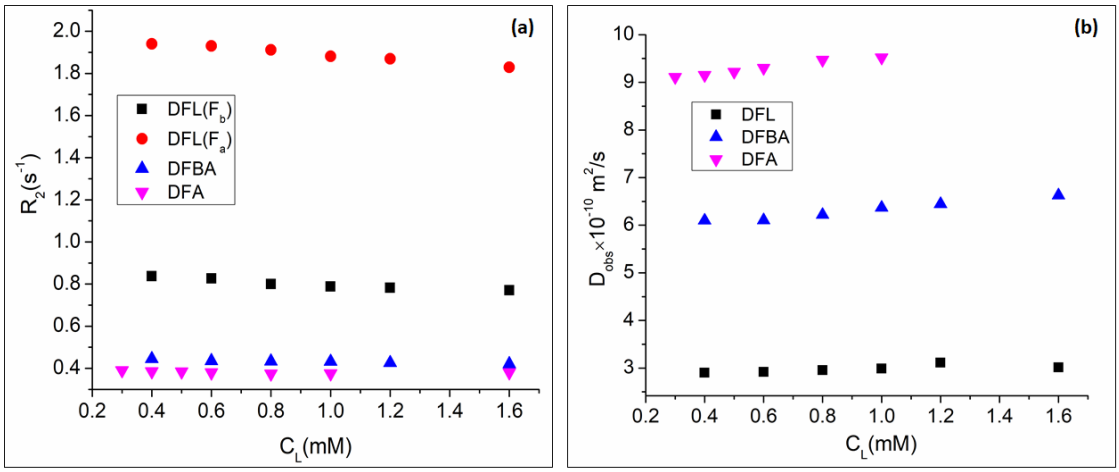

Figure 3.15: Plot of measured ^{19}F (a) relaxation rate (R_2) and (b) self-diffusion coefficient (D) of ligand DFL, DFBA, and DFA for varying concentration of ligands in the presence of 10 μM trypsin recorded at 298 K and pH=7.40.

It can be seen from the plots that there are no change in the values of measured R_2 and D for these fluorochemicals in presence of trypsin compared to the free fluorochemicals. Therefore, it is not meaningful to address these plots further. Consequently it can be interpreted that fluorochemicals with mainly carboxylic acid as functional group (DFL, DFBA, DFA) do not show any interaction of significant magnitude with trypsin.

3.4 CONCLUSIONS

The investigation reported in the present chapter (both part I and II) allows us to exhibit that a complete set of 1D ligand-based NMR methods is sufficient to provide a detailed quantitative analysis of a fluorinated ligand-protein complex as well as such analysis points out lack of interaction between ligand and protein unambiguously. Two powerful NMR experiments *viz*., transverse relaxation, and diffusion are employed to analyse the ligand-protein interaction in solution. Further, we also attempted to compare the applicability of these methods in terms of their ease of implementation as well as amount of information revealed. An initial confirmation of binding interaction is achieved from the measurement of line-broadening that indicated ^{19}F T_2 being more potent than ^{19}F T_1 and ^{1}H T_2 measurement in similar cases. This is attributed to a more significant contribution of chemical shift anisotropy mediated transverse relaxation mechanism in case of ^{19}F.

It should be highlighted that both NMR relaxation-based measurements and NMR diffusion-based measurements allow the quantitative determination of K_D. However, these two methods have their pros and cons. Acquisition of relaxation data is less demanding in terms of NMR hardware, whereas to generate diffusion data, one would need to have a provision of application of pulsed-field gradients. On the other hand, relaxation rates being governed by local dynamics of the molecule could be difficult to decipher while self-diffusion coefficient is more like a global parameter and would be able to reflect the effect of the protein binding in totality [Luo et al., 1999]. Since, relaxation data is site dependent, two different K_D values have been extracted from relaxation based measurements in case of DFL while a single K_D value is obtained from diffusion measurements of the DFL–HSA system as seen in table 3.4 (part I of current study). Although, relaxation based analysis could become cumbersome due to local molecular motion, it represents the binding with more specificity by indicating the most affected parts of the molecule exhibiting highest changes in their relaxation rates. A similar discussion for DFBA–BSA is not required as molecule DFBA contains only one type of fluorine.

On the other hand, ligand detected STD experiments are robust in understanding the mode and mechanism of ligand binding with the help of GEM. STD experiments also enable determination of site dependent binding constants, albeit the limitation is in terms of long experimental time and less sensitivity. STD NMR pulse sequences require specialized modifications alongwith use of gradients. Also, STD NMR is limited in probing binding parameters associated with high-affinity complexes. Therefore, in the present study, relaxation and diffusion based measurements are preferred over STD to extract binding parameters.

In Part I, constant time fast pulsing CPMG is employed to extract the two site exchange rate (K_{ex}) between the free and bound state of the ligand. The related kinetic parameters, *i.e*., K_{off} and τ_{res} are also determined. This method provides number of advantages, *viz*., quick acquisition at natural abundance, requirement of nominal sample concentration, possibility of variation of the concentration ratio of protein: ligand to a larger extent and ease of implementation. The relevant kinetic parameters of the ligand binding event have been experimentally determined from the different ^{19}F NMR methods. The dissociation constants and number of binding sites are determined from diffusion and T_2 values of the ligand. The values suggest the binding is weak and non-specific in nature. It must be mentioned here that in general it is considered in literature that the systems in fast exchange are weak binders. The binding site determination experiments also indicate about the non-specific nature of binding between DFBA–BSA. All the

methods employed to analyse the binding kinetics are in good agreement and confirms the applicability of two site exchange model. The bound fraction calculated in all the cases indicated saturation of protein binding sites with increasing ligand concentrations. Therefore a complete analysis of DFBA–BSA interaction and comparison with similar molecular system DFL–HSA has been accomplished with an exclusive application of ^{19}F NMR methods. Furthermore, DFBA–BSA molecular interaction has potential to be extrapolated to analyze interaction between protein and large fluorinated molecules that are insoluble in aqueous media and are either prepared from or degrade to DFBA. Moreover, dissociation constant and half-life of the ligand-protein complex have always been of great interest in pharmaceutical industries as these parameters affect the delivery of molecule to target tissues. If the binding is too strong, the availability of that ligand in the plasma will be reduced and hence leading to slower diffusion of the ligand to the target [Dahiya et al., 2017]. Because of their slow distribution, a high dose of these drugs will be required *in vivo* for their efficient mode of action at target tissues [Ghuman et al., 2005]. Also, there is a chance of accumulation of these molecules in plasma as they may not get efficiently eliminated. On the other hand, the weak binding will ensure ease of circulation and timely excretion of the drug from the body. Therefore, it is essential to identify drug molecules with moderate binding to carrier SA. In our case, DFBA is found to be weaker binder than DFL, hence it can be speculated that DFBA will experience greater diffusion to target tissues than DFL due to increased bio-availability. These kind of studies can provide a valuable insight in understanding the pharmacokinetics between ligand and target protein pair [Liu et al., 1997].

The study conducted in part-II further extended the potential applicability of established ^{19}F 1D NMR methods for Part I to probe the binding interactions between the organofluorine and trypsin system. In part II, it is found that fluorinated molecules having carboxylic acid functional groups (DFL, DFBA, DFA) do not show any detectable binding affinity towards trypsin. It suggests that the structure of the binding molecule and nature of the active binding site of protein plays an essential role in the association dynamics and binding mechanism of ligands with proteins. This study is pivotal in terms of knowledge about the effects of these organofluorines on digestive enzymes.

…